

Bulk photovoltaic effect in an organic polar crystal†

 Cite this: *Chem. Commun.*, 2014, 50, 6530

 Received 17th February 2014,
 Accepted 3rd May 2014

DOI: 10.1039/c4cc01255k

www.rsc.org/chemcomm

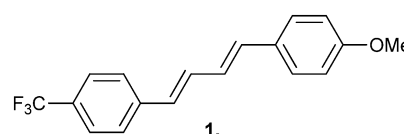
 Ratheesh K. Vijayaraghavan,^a Stefan C. J. Meskers,^{*ab} M. Abdul Rahim^c and Suresh Das^c

Organic polar crystals from the donor–acceptor substituted 1,4-diphenylbutadiene **1** can generate a short-circuit photocurrent and a photovoltage upon illumination with near UV light. The photocurrent and photovoltage are attributed to a bulk photovoltaic effect. The bulk photovoltaic effect has been known for inorganic polar crystals for decades and can now also be demonstrated for organic polar crystals.

The bulk photovoltaic effect involves the spontaneous generation of photocurrent and photovoltage upon illumination of a spatially uniform material. Because the spontaneous photocurrent and the photovoltage have vectorial character, Curie's symmetry principle states that the bulk photovoltaic effect can only occur in *polar* materials.

For polar inorganic crystals, the bulk photovoltaic effect is well known.¹ The bulk photovoltaic effect has recently received renewed interest, partly because of the possibility to make photovoltaic cells that can generate open circuit voltages that by far exceed the bandgap of the semiconducting active layer.² In fact open circuit voltages up to several kV have been reported.³ The bulk photovoltaic effect can be explained qualitatively by generation and separation of photogenerated charge carriers under the influence of the internal or built-in electric field that exists in any bulk polar crystal.

Although the bulk photovoltaic effect in *inorganic* ferroelectric crystals is by now well established, for *organic* crystals the bulk photovoltaic effect has not been addressed yet. Recently it has


 Chart 1 Chemical structure of **1**.

been shown that large photovoltages can be generated in crystals of the biomacromolecules constituting the plant photosystem I.⁴ Furthermore, photovoltaic action in a poled organic material has recently been demonstrated.⁵ Study of bulk photovoltaic effects in crystals of organic molecule is hampered by the difficulty in obtaining organic polar crystals with absorption in the appropriate spectral range and sufficient charge transport properties.⁶

Here we investigate the 1,4-diphenylbutadiene derivative **1** (Chart 1), carrying an electron donating methoxy- and an electron withdrawing trifluoromethyl-substituent.⁷ The asymmetric substitution introduces donor–acceptor character and results in a considerable static dipole moment for **1**, determined to be 3.8 Debye in dioxane solution. The dipolar vector is oriented along the long axis of the molecule.

The compound **1** was synthesized *via* the Wittig–Horner–Emmons reaction (see ESI† for further details). Single crystals of the molecule were obtained from a toluene-chloroform mixture. Analysis of X-ray diffraction data for a single crystal of **1** revealed the orthorhombic crystal system with *Pca2*(1) space group. The *Pca2*(1) space group allows for polar crystals. The crystal consists of regular herringbone stacks with four molecules per unit cell (Fig. 1). The molecules are almost planar with the plane of phenyl rings making only a small 4.7° dihedral angle with the plane of the central butadiene unit. The planarity warrants conjugation of the π -electrons over the entire molecule. The long axis of all four of the molecules in the unit cell lie parallel to the *ac* plane and make a $\pm 32^\circ$ angle with the *c* axis (Fig. 2). In the direction of the *a*- or *b*-axis, the components of the dipole moments of the four molecules in the unit cell cancel each other. In the *c*-direction, the dipole moments add up to a net static polarization.

^a Molecular Materials and Nanosystems, Eindhoven University of Technology, PO Box 513, 5600 MB Eindhoven, The Netherlands. E-mail: s.c.j.meskers@tue.nl

^b Institute for Complex Molecular Systems, Eindhoven University of Technology, The Netherlands

^c Photosciences and Photonics, Chemical Sciences and Technology Division, National Institute for Interdisciplinary Science and Technology (CSIR), Trivandrum, India

† Electronic supplementary information (ESI) available: Detailed synthetic procedures and characterization, single crystal X-ray analytical data and experimental techniques are available. CCDC 987360. For ESI and crystallographic data in CIF or other electronic format see DOI: 10.1039/c4cc01255k

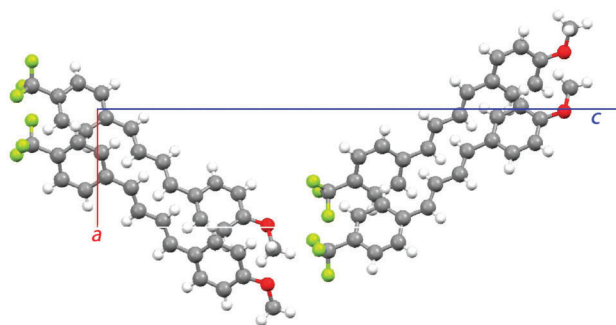


Fig. 1 Unit cell for a single crystal of **1** from X-ray diffraction analysis with four molecules per unit cell.

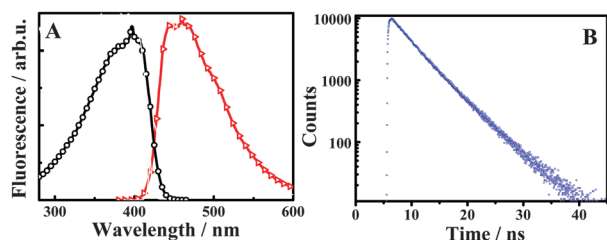


Fig. 2 (A) Fluorescence (red) and fluorescence excitation (black) spectra for a single crystal of **1**. (B) Fluorescence decay profile of a single crystal of **1**. Excitation at 400 nm, emission collection at 480 nm.

Crystals of **1** show bright blue fluorescence, with maximum around 460 nm (Fig. 2A) upon excitation with light with wavelength shorter than 420 nm (see Fig. 2A). The fluorescence decays almost monoexponentially with a lifetime of around 5.2 ns (Fig. 2B). The monoexponential decay and the limited Stokes shift of the fluorescence in the solid, indicate the absence of severe exciton self-trapping and/or excimer formation in the crystalline state.

Fluorescence polarization microscopy shows that absorption of light by crystals of **1** is highly polarized. Consistent with the

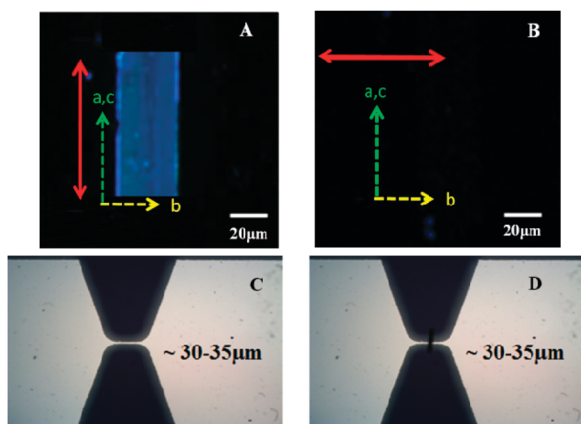


Fig. 3 (A, B) Polarized fluorescence microscope images of a single crystal of **1**. Red arrows indicate the direction of polarization of excitation. (C) Transmission optical microscope image of the gold electrodes used to measure the photovoltaic effect with spacing of 30–35 μm . (D) Image taken after depositing the crystal of **1** having $\sim 50 \times 30 \times 100 \mu\text{m}^3$ dimension.

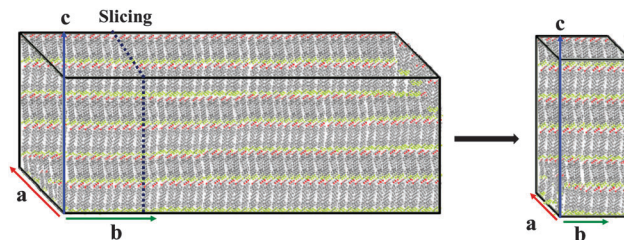


Fig. 4 Slicing of as-grown single crystals of **1** into smaller sections for oriented insertion between electrodes.

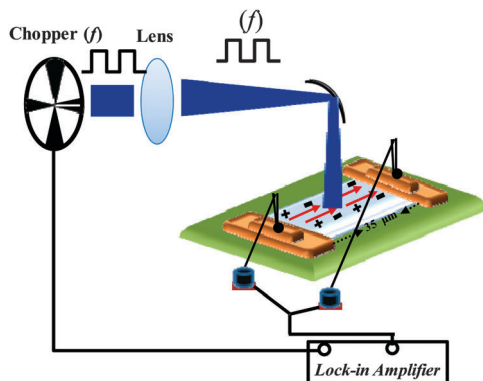
packing as determined from analysis of the X-ray diffraction, the fluorescence vanishes when the excitation light is polarized parallel to the crystal *b*-axis.

Fluorescence spectroscopy on isolated molecules of **1** in polar solvent, indicate that the dipole moment of **1** in the lowest singlet excited state (11.3 Debye) is higher than in the ground state (3.8 Debye). The fluorescence band shows a large solvatochromic red shift that increases with increasing solvent polarity.⁷ This is consistent with net photoinduced transfer of charge from the side of the molecule bearing the methoxy substituent to the side carrying the fluoromethyl group. Importantly, because of the alignment of the molecules of **1** in the crystal, photoexcitation of the crystal will result in a net transfer of charge from one side of the crystal to the other along the crystallographic *c*-axis.

In order to measure this photoinduced transfer of charge in the polar crystal, we have mounted crystals of **1** in between two gold electrodes, see Fig. 3D. For electrical detection of a photoinduced potential difference between the electrodes, the orientation of the crystal with respect to the electrodes is of prime importance. The *c*-axis of the crystal that corresponds to the net direction of charge transfer, needs to point in the same direction as the shortest line between the edges of the two electrodes used for measuring the photovoltage. Because the crystals are plate-like, growing fastest in the *b* direction, we sliced the as-grown crystals into smaller parts that could be oriented with their *c*-axis in the direction of the electrode spacing (Fig. 4).

Gold electrodes with 30–35 μm spacing were fabricated by thermal sublimation of the metal onto glass through a mask. A 5 nm Cr adhesion layer was applied between glass and gold to strengthen binding of the metal. The thickness of the electrodes was approx. 100 nm. Electrical contact between crystal and gold electrode was reinforced using conducting epoxy resin containing silver. The crystal was illuminated with light of 364 nm from a continuous wave argon ion laser. The light from the laser was modulated mechanically by a chopper. Alternating photocurrents and voltages were measured separately using a lock-in amplifier (Stanford SR830, 10 M Ω input impedance) as function of frequency of modulation and intensity of the incoming light (Scheme 1). All the measurements were carried out under normal atmospheric condition. We stress that in the photocurrent measurements no external voltage is applied to the crystals.

We find that single crystals of **1** can generate a spontaneous photocurrent and a photovoltage under illumination with UV light, see Fig. 5. Photocurrent and photovoltage dependent



Scheme 1 Schematic representation of the experimental set-up for the photocurrent and photovoltage measurement.

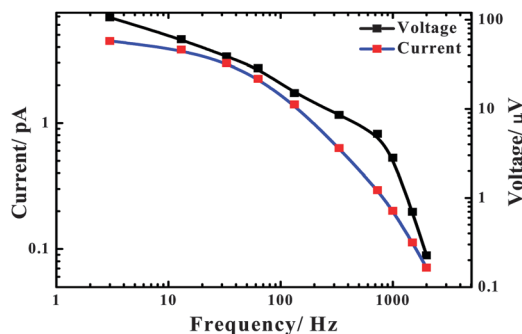


Fig. 5 Modulation frequency dependence of the spontaneous, short-circuit photocurrent and photovoltage.

on the modulation frequency of the incident light beam. At frequencies above 10^2 Hz, both current and voltage rapidly decrease with increasing frequency. The magnitude of the photovoltage was found to decrease from ~ 100 μV at 3 Hz to nearly ~ 88 nV at 3.3 kHz. The corresponding change in current was from 4.4 pA to 0.07 pA. The frequency dependence indicates a transport limitation in the built-up and recombination of photogenerated charge.

Fig. 6 illustrates the dependence of spontaneous photocurrent and photovoltage on the intensity of the incident laser light expressed as power. The power of illumination was varied from 3 mW to 95 mW. Beyond this flux density, the sample found to undergo decomposition with black dots appearing in the crystal, indicative of charring. At low power, the short circuit current density varies approximately linearly with the power. At high intensity, a superlinear, quadratic dependence of the spontaneous photocurrent on power is observed. The photovoltage shows a dependence on power that is steeper than for the current and also shows a crossover for a low intensity to a high intensity regime at about 30 mW. The monochromatic power conversion efficiency is low, on the order of 10^{-12} . The superlinear dependence of short-circuit current on illumination intensity indicates that photocarrier generation and collection involving sequential absorption of two photons is more efficient than the corresponding processes driven by a single photon. Two photon absorption is rather unlikely under CW

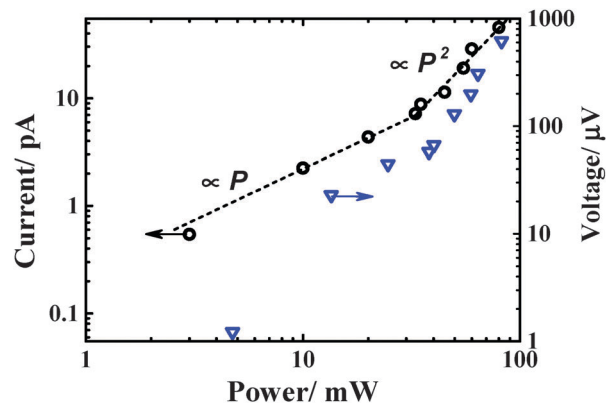


Fig. 6 Dependence of spontaneous photocurrent and photovoltage generated by a single crystal of **1** on power of the illuminating laser beam. The dashed lines indicate linear and quadratic power dependencies.

illumination, exciton-exciton annihilation type processes are however likely to occur.

The superlinear photocurrent provides an indication against thermal effects as the source of the photovoltaic effect. Thermal gradients are linear or sublinear in the heating power. Inhomogeneous illumination of semiconductors can lead to a photo-Dember effect,⁹ as the result of an asymmetric carrier generation profile in combination with a difference in diffusion constant for n and p-type carriers. The lateral electrode structures used here allow for homogenous illumination, minimizing the photo-Dember effect. Moreover the photo-Dember effect in organic diodes is (sub-)linear in illumination intensity,¹⁰ whereas the effect under study shows superlinear behavior.

Finally, in a polar organic crystal in which the dipole moment of the molecules changes upon photoexcitation, illumination with intensity modulated excitation light should yield an alternating current due to a light-induced change in the net polarization of the crystal.⁸ The relevant timescale for this transient current is the excited state lifetime (5.2 ns). Near the start and end of each illumination period, a fixed amount of charge ΔQ will be exchanged *via* the electrodes within a time window of about 5 ns. The polarization related alternating photocurrent I_p , should increase in magnitude with increasing frequency because $I_p = \Delta Q/T = \nu \Delta Q$ with T the period and ν the frequency of the modulation. In our experiment, we use low modulation frequencies, limiting the contribution of this polarization related current. Moreover the experimentally determined photocurrent decreases with increasing frequency, whereas the polarization mechanism predicts an increase with frequency. The frequency and intensity dependence observed indicate photogeneration of charge carrier involving multiple excitons combined with asymmetric charge transport in the polar crystal.

In summary, we find experimental evidence for a bulk photovoltaic effect in a polar crystal of a donor-acceptor substituted π -conjugated molecule.

This work is part of the Joint Solar Programme (JSP) of Hyet Solar and the Stichting voor Fundamenteel Onderzoek der Materie FOM, which is part of The Netherlands Organisation for Scientific Research (NWO). The work has received funding

from the Ministry of Education, Culture and Science (Gravity program 024.001.035).

Notes and references

- 1 (a) A. G. Chynoweth, *Phys. Rev.*, 1956, **102**, 705–714; (b) F. S. Chen, *J. Appl. Phys.*, 1969, **40**, 3389–3396; (c) A. M. Glass, D. Von der Linde and T. J. Negran, *Appl. Phys. Lett.*, 1974, **25**, 233–235.
- 2 (a) S. Y. Yang, J. Seidel, S. J. Byrnes, P. Shafer, C.-H. Yang, M. D. Rossell, P. Yu, Y.-H. Chu, J. F. Scott, J. W. Ager, L. W. Martin and R. Ramesh, *Nat. Nanotechnol.*, 2010, **5**, 143–147; (b) T. Choi, S. Lee, Y. J. Choi, V. Kiryukhin and S.-W. Cheong, *Science*, 2009, **324**, 63–66; (c) W. Ji, K. Yao and Y. C. Liang, *Adv. Mater.*, 2010, **22**, 1763–1766; (d) I. Grinberg, D. V. West, M. Torres, G. Gou, D. M. Stein, L. Wu, G. Chen, E. M. Gallo, A. R. Akbashev, P. K. Davies, J. E. Spanier and A. M. Rappe, *Nature*, 2013, **503**, 509–512.
- 3 W. T. H. Koch, R. Munser, W. Ruppel and P. Wurfel, *Solid State Commun.*, 1975, **17**, 847–850.
- 4 H. Toporik, I. Carmeli, I. Volotsenko, M. Molotskii, Y. Rosenwaks, C. Carmeli and N. Nelson, *Adv. Mater.*, 2012, **24**, 2988–2991.
- 5 R. Castagna, M. Garbugli, A. Bianco, S. Perissinotto, G. Pariani, C. Bertarelli and G. Lanzani, *J. Phys. Chem. Lett.*, 2012, **3**, 51–57.
- 6 R. Glaser, *Acc. Chem. Res.*, 2007, **40**, 9–17.
- 7 V. Alain, S. Rédoglia, M. Blanchard-Desce, S. Lebus, K. Lukaszuk, R. Wortmann, U. Gubler, C. Bosshard and P. Günter, *Chem. Phys.*, 1999, **245**, 51–71.
- 8 M. Garbugli, M. Porro, V. Roiati, A. Rizzo, G. Gigli, A. Petrozza and G. Lanzani, *Nanoscale*, 2012, **4**, 1728–1733.
- 9 H. Dember, *Phys. Z.*, 1931, **32**, 554–557.
- 10 D. Sarkar and N. J. Halas, *Solid State Commun.*, 1994, **90**, 261–265.